



# What potential do mosses have as biomonitors of POPs? A comparative study of hexachlorocyclohexane sorption

Z. Chaos<sup>a,\*</sup>, J.A. Fernández<sup>b</sup>, M. Balseiro-Romero<sup>a</sup>, M. Celeiro<sup>c</sup>, C. García-Jares<sup>c</sup>, A. Méndez<sup>a</sup>, P. Pérez-Alonso<sup>a</sup>, B. Estébanez<sup>d</sup>, J. Kaal<sup>e</sup>, K.G.J. Nierop<sup>f</sup>, J.R. Aboal<sup>b</sup>, C. Monterroso<sup>a</sup>

<sup>a</sup> CRETUS, Dept. Edafología e Química Agrícola, Universidade de Santiago de Compostela, 15782 Santiago de Compostela, Spain

<sup>b</sup> CRETUS, Ecology Unit, Universidade de Santiago de Compostela, 15782 Santiago de Compostela, Spain

<sup>c</sup> CRETUS, Dept. Química Analítica, Nutrición e Bromatología, Universidade de Santiago de Compostela, 15782 Santiago de Compostela, Spain

<sup>d</sup> Dept. Biología, Unidad de Botánica, Universidad Autónoma de Madrid, 28049 Madrid, Spain

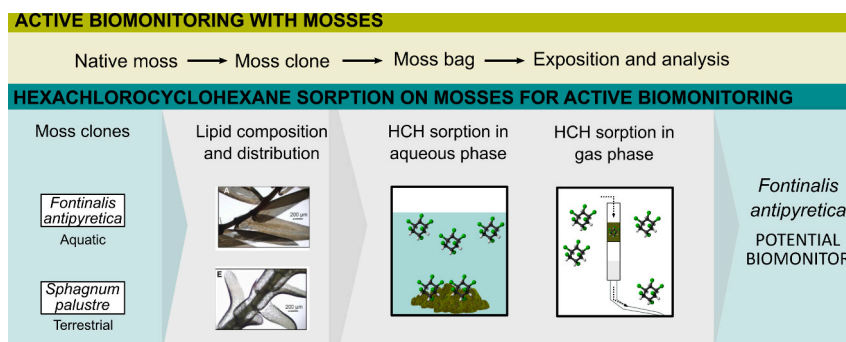
<sup>e</sup> Pyrolyscience, 15707 Santiago de Compostela, Spain

<sup>f</sup> Geolab, Faculty of Geosciences, Utrecht University, Princetonlaan 8, 3584 CB Utrecht, the Netherlands

## HIGHLIGHTS

- Gas-phase HCH biosorption evaluated by a new solid phase extraction method.
- *F. antipyretica* showed more lipids in chromatograms and cell wall staining.
- In aqueous medium *F. antipyretica* retained 5 mg g<sup>-1</sup> HCHs and *S. palustre* 1 mg g<sup>-1</sup>.
- In gas medium *F. antipyretica* retained 113 % HCHs and *S. palustre* 32 %.
- *F. antipyretica* is suggested as a potential biomonitor of HCHs.

## GRAPHICAL ABSTRACT



## ARTICLE INFO

Editor: Paromita Chakraborty

### Keywords:

Biomonitoring  
*Sphagnum palustre*  
*Fontinalis antipyretica*  
 Persistent organic pollutant  
 Lindane

## ABSTRACT

Persistent organic pollutants (POPs) pose a significant global threat to human health and the environment, and require continuous monitoring due to their ability to migrate long distances. Active biomonitoring using cloned mosses is an inexpensive but underexplored method to assess POPs, mainly due to the poor understanding of the loading mechanisms of these pollutants in mosses. In this work, *Fontinalis antipyretica* (aquatic moss) and *Sphagnum palustre* (terrestrial moss) were evaluated as potential biomonitors of hexachlorocyclohexanes (HCHs:  $\alpha$ -,  $\beta$ -,  $\gamma$ -,  $\delta$ -HCH), crucial POPs. Moss clones, grown in photobioreactors and subsequently oven-dried, were used. Their lipid composition and distribution were characterized through molecular and histochemical studies. Adsorption experiments were carried out in the aqueous phase using the repeated additions method and in the gas phase using an active air sampling technique based on solid-phase extraction, a pioneering approach in moss research. *F. antipyretica* exhibited greater lipid content in the walls of most cells and higher adsorption capacity for all HCH isomers in both gaseous and liquid environments. These findings highlight the need for further

\* Corresponding author.

E-mail address: [mzoe.chaos@usc.es](mailto:mzoe.chaos@usc.es) (Z. Chaos).

<https://doi.org/10.1016/j.scitotenv.2024.173021>

Received 18 January 2024; Received in revised form 3 May 2024; Accepted 4 May 2024

Available online 11 May 2024

0048-9697/© 2024 The Authors. Published by Elsevier B.V. This is an open access article under the CC BY-NC license (<http://creativecommons.org/licenses/by-nc/4.0/>).

investigation of POP loading mechanisms in mosses and open the door to explore other species based on their lipid content.

## 1. Introduction

In the current context of global climate change, pollution stands out as a significant driver, with persistent organic pollutants (POPs) posing particular concern. POPs are considered “silent killers” and are present in all environments, causing lethal diseases and environmental problems (see e.g. Alharbi et al., 2018). These compounds include the hexachlorocyclohexane (HCH) isomers  $\alpha$ -,  $\beta$ - and  $\gamma$ -HCH (UNEP, 2009), which were commercialised as pesticides in two formulations, technical grade HCH (from 1940 to 1970) and lindane (from 1970 to early 2000). The prolonged use of these compounds resulted in the largest legacy of POP contamination to date.

The technical grade HCH was a mixture of isomers and was later refined to produce lindane, consisting of 99 %  $\gamma$ -HCH, the sole isomer with insecticidal properties. However, lindane production is highly inefficient, with 8–12 t of waste produced per tonne of lindane. Between 1950 and 2000, an estimated 4–7 million tonnes of HCH waste, mainly  $\alpha$ - and  $\beta$ -HCH, were haphazardly dumped in open sites known as mega-sites (Vijgen et al., 2011). Once introduced into the environment, these compounds are more easily dispersed than other organochlorine pesticides (e.g. DDT) in all environmental compartments, posing a threat to humans and the environment (Vega et al., 2016; Kim et al., 2017; Vijgen et al., 2018). Most countries have prohibited its use and production and, in some cases, have invested great economic efforts in the remediation of localised mega-sites, as is the case of Spain, where the first base-catalyzed dechlorination plant was installed in treating lindane (Vijgen et al., 2019). The economic cost of these technologies prevents some countries from investing in the remediation of soils contaminated with HCH or from opting for cheaper methods, such as soil encapsulation. The scientific community continues to strive to find cost-effective and sustainable alternatives for complete HCH removal, such as bioremediation (Usmani et al., 2021) or nanoremediation (Fei et al., 2022). While the direct release of HCH into the environment has decreased greatly, HCH continues to persist in the environment, e.g. in soils (Ma et al., 2020), plants (Łozowicka et al., 2016), freshwater systems (Singh et al., 2023) or air (Halvorsen et al., 2023) and disperses to locations far from the source of contamination (Hao et al., 2021; Wong et al., 2021). Furthermore, the effects of climate change may increase the mobility of this pollutant and lead to an imbalance in primary and secondary emissions (Ma et al., 2011; Wöhrnschimmel et al., 2012; Halvorsen et al., 2023).

Given the persistence and mobility of HCH, coupled with the influence of climate change, monitoring is essential to understand the behaviour of the pollutant in the environment and to effectively manage its spatio-temporal evolution. In Europe, monitoring of HCH in air and water is required under the EMEP (European Monitoring and Evaluation Programme; <https://www.emep.int/>) (Tørseth et al., 2012) and the WFD (Water Framework Directive) (Directive 2000/60/EC). However, these measures are not sufficient to establish global trends, and monitoring at higher spatial resolution is needed (Wöhrnschimmel et al., 2012; Halvorsen et al., 2023).

Biomonitoring, which involves using living organisms, is a valuable tool for assessing environmental pollution and can complement traditional monitoring approaches to obtain higher spatial resolution. Mosses are widely distributed and can accumulate various pollutants with high tolerance, so native mosses have been used for biomonitoring heavy metals (>369 articles; Boquete et al., 2017), and POPs (mainly for polycyclic aromatic hydrocarbons – PAHs – and, to a lesser extent, for other compounds such as organochlorines, dioxins and furans) (Harmens et al., 2013), although in smaller numbers (a few tens of articles). Even fewer studies have considered HCH (i.e. Holoubek et al., 2000;

Borghini et al., 2005; Lim et al., 2006; Tarcau et al., 2013; Zhu et al., 2015). However, the required spatial resolution would only be achieved by applying active biomonitoring using transplanted mosses (“moss-bags”); for further details about this technique and its standardization, see Ares et al. (2012). The use of transplanted mosses allows the required sampling density to be reached and also the selection of appropriate monitoring sites, providing more accurate measurements at higher spatial resolution than would be possible using conventional techniques (Pacín et al., 2023). On the other hand, the relationship between the concentration of POPs in the atmosphere and in mosses has only been studied using transplanted mosses –specifically for PAHs– with very satisfactory results (see details in Aboal et al., 2020). To date, transplanted mosses have rarely been used for biomonitoring POPs (until 2012: 4 times for PAHs and once for PCBs, Ares et al., 2012; with very few additions since then and never before for monitoring HCHs).

In the last decade, great efforts have been made to standardize active biomonitoring with mosses, including the production of clones of some species (e.g. Ares et al., 2012; Beike et al., 2015; Capozzi et al., 2017). However, these efforts mainly apply to heavy metal monitoring, for which different species have been recommended. *Sphagnum palustre* L. was proposed for active biomonitoring of atmospheric pollution (Ares et al., 2012), and a clone was produced (Beike et al., 2015). *Fontinalis antipyretica* Hedw. was recommended for active biomonitoring of water pollution (Debén et al., 2017) and later the corresponding clone was also recommended (Debén et al., 2019). In addition, although the process of heavy metal loading by mosses has been well studied (e.g. González and Pokrovsky, 2014; González et al., 2016; García-Seoane et al., 2023; Varela et al., 2023), the POP loading process in mosses remains unknown. Only a general, theoretical study (Harmens et al., 2013) and some partial studies, e.g. for phenanthrene (Keyte et al., 2009; Spagnuolo et al., 2017), have been conducted. Unfortunately, little or no attention has been paid to the effect of lipid composition in relation to the loading capacity, although it is known to be the main factor responsible for the loading of aqueous or volatile forms of these pollutants. This gap in the knowledge of loading mechanisms has made it difficult to prioritise the selection of moss species for POP biomonitoring.

The main objective of the present study was to evaluate the efficiency of the available moss clones (*F. antipyretica* and *S. palustre*) in adsorbing HCHs ( $\alpha$ -,  $\beta$ -,  $\gamma$ - and  $\delta$ -isomers) for their use as biomonitors in aquatic and gaseous environments. We investigated the HCH retention capacity of mosses, and we also considered whether aquatic mosses might perform better in aquatic environments and terrestrial mosses in gaseous environments. A further aim of the study was to obtain more information about the loading of HCH (as an example of POPs) and about which characteristics of mosses (i.e. composition and lipid localisation) contribute to maximising HCH accumulation. Finally, we hope that this information could be used to identify the best moss species for active biomonitoring of POPs.

## 2. Material and methods

### 2.1. Moss material

Moss clones were grown in photobioreactors under axenic conditions in the Laboratory of the Ecotoxicology and Plant Ecophysiology Research Group, University of Santiago de Compostela. The conditions for producing and growing the mosses have been described by Debén et al. (2019) for *F. antipyretica* and by Beike et al. (2015) for *S. palustre*. Briefly, clones were cultured in 12 L photobioreactors (Bio Bundle 15 M Applikon, Delft, The Netherlands) with modified liquid Knop medium.

The bioreactors were illuminated and aerated continuously and subjected to temperature and sterility controls. For the biosorption experiments, both moss clones were devitalized by oven-drying with a moss-specific temperature ramp to prevent interference with metabolism and to produce more stable results (e.g. [Debén et al., 2017](#)).

## 2.2. Characterization of moss material

The material used was characterized in order to determine how the composition (molecular characterization) and location (histochemical characterization) of the lipids in mosses could explain the results of the adsorption experiments.

### 2.2.1. Molecular characterization

Molecular characterization of moss tissues was performed by a combination of the following: 1) pyrolysis-gas chromatography-mass spectrometry (Py-GC-MS) of solid samples; 2) thermally assisted hydrolysis and methylation-GC-MS (THM-GC-MS) of solid samples; and 3) GC-MS of total lipid extracts. Samples were ground in a ball mill (RETSCH MM 400). Pyrolysis-GC-MS was performed using a Pyroprobe 5000 pyrolyzer (CDS Analytical) coupled to a 5977 GC-MS system (Agilent Technologies). The pyrolysis set-point temperature was 650 °C (10 s, 10 °C ms<sup>-1</sup> heating rate). The pyrolysis interface, GC inlet and GC-MS interface were held at 325 °C. The GC oven was heated from 60 °C (1 min hold) to 325 °C (3 min hold) at a rate of 20 °C min<sup>-1</sup>. The GC was operated in 1:25 split mode and was equipped with an HP5-MS column. The helium carrier flow was 1 mL min<sup>-1</sup>. The detector scanned in the *m/z* 50–500 range. Prior to inclusion of the sample for THM-GC-MS analysis, an aliquot of 25 % aqueous tetramethylammonium hydroxide (TMAH) was added. The oven temperature was increased from 70 °C (3 min hold) to 325 °C (5 min hold) at a rate of 20 °C min<sup>-1</sup>.

For GC-MS analysis of total lipid extracts (TLEs), the samples were extracted for 24 h with dichloromethane (DCM) and methanol (9:1; v/v) in a Soxhlet apparatus. The TLEs obtained were dried over Na<sub>2</sub>SO<sub>4</sub>, and the solvent was then evaporated under N<sub>2</sub>. The TLE was methylated with trimethylsilyldiazomethane to convert acid groups into corresponding methyl esters, purified over a SiO<sub>2</sub> column, and silylated with bis(trimethylsilyl)trifluoroacetamide (BSTFA) in pyridine at 60 °C for 20 min to convert the hydroxy groups into the corresponding trimethylsilyl (TMS) ethers. Prior to GC-MS analysis, all aliquots were dissolved in ethyl acetate. The TLEs were on-column injected in a CP-sil 5CB fused silica column (30 m × 0.32 mm i.d., film thickness 0.10 µm) in an Agilent 7890B GC 5977B platform. The GC-MS was operated at a constant flow of 1.0 mL min<sup>-1</sup>. The oven temperature was increased from 70 °C to 130 °C at a rate of 20 °C min<sup>-1</sup> and then to 320 °C at a rate of 4 °C min<sup>-1</sup>, followed by an isothermal hold for 20 min. The MS was operated in full data acquisition mode, scanning ions from *m/z* 50–800.

### 2.2.2. Histochemical characterization

Mosses were histochemically characterized for internal lipids and external wax-like substances with the Sudan Black B test ([Jensen, 1962](#)). Whole shoots were briefly held (ca. 2 min) in 50 % ethanol in an Eppendorf tube, before being transferred to another tube filled with a saturated, filtered solution of Sudan Black B (Fluka 86015) in 70 % ethanol, held for 5 min, before being differentiated in 50 % ethanol. Lipophilic substances (lipid droplets, plastoglobuli and external wax-like compounds) stain dark blue-black. The samples were mounted in 50 % ethanol for microscopic observation with an Olympus BX61 microscope, and photographs were taken with an Olympus DP70 camera.

## 2.3. Liquid phase batch biosorption experiment

The adsorption isotherm data were obtained in batch-type experiments by using the method of repeated additions suggested by [Bowman \(1979\)](#) for low-solubility pesticides. For the consecutive additions, solutions of a mixture of HCH isomers were prepared in bi-distilled water

from the stock solutions of each isomer (see supplementary material, SM.1.). The concentration of each isomer was lower than the solubility limit previously determined by [Rodríguez-Garrido \(2009\)](#). The concentrations were approximately 1 mg L<sup>-1</sup> α-HCH, 0.1 mg L<sup>-1</sup> β-HCH and 2 mg L<sup>-1</sup> of γ-HCH and δ-HCH, totalling about 5 mg L<sup>-1</sup> of the sum of the isomers (ΣHCH). In addition, 5 mM NaN<sub>3</sub> was added to eliminate any possible effect of microorganisms, and 5 mM CaCl<sub>2</sub> was added as a background electrolyte. Prior to each addition, the HCH concentration was measured in triplicate. For the experiment, the mosses (50 mg each) were immersed in 25 mL of the mixed HCH isomers, NaN<sub>3</sub> and CaCl<sub>2</sub> solution in 100 mL glass flasks closed with PTFE caps and tightly sealed with Parafilm®. The moss suspensions were stirred for 24 h in a back-and-forth shaker (< 100 rpm) at room temperature (ca. 20 °C) in darkness. This length of time was previously determined to be sufficient to reach equilibrium ([Rodríguez-Garrido, 2009](#)). Subsequently, 20 mL of the liquid phase was removed with a glass pipette, and another 20 mL of the mixed HCH isomers, NaN<sub>3</sub> and CaCl<sub>2</sub> solution were added before analysis. This step was repeated until the measured concentration remained constant. Five replicates of the moss suspensions were measured, and a moss-free solution subjected to the same repeated additions was included as a control. For quantification of the equilibrium concentration of HCH isomers, the compounds were extracted with 5 mL of hexane (1:1 v/v) for 20 min in Pyrex® tubes in an ultrasound bath (Ultrasons J. P. Selecta SA). This technique yields recovery rates >95 % ([Concha-Graña et al., 2004](#)). The extracts obtained were then analyzed in a GC-MS-system (Model 450 GC, Model 220 MS Agilent Technologies) equipped with a Combi-PAL autosampler (CTC-Analytics, AG, Switzerland). The system was operated in electron impact mode, with tandem mass spectrometry as the detection mode. The helium carrier flow was 1 mL min<sup>-1</sup>. The volume of the extracts injected was 1 µL and the injector operated at 280 °C in pulsed split/splitless mode. The GC oven temperature programme was 80 °C (1.5 min), 30 °C min<sup>-1</sup> to 180 °C (1 min), 3 °C min<sup>-1</sup> to 200 °C and 40 °C min<sup>-1</sup> to 290 °C. The calibration line was obtained using standards (1–5000 µg L<sup>-1</sup>) prepared in hexane, and IS was added to both extracts and calibration standards at a concentration of 250 µg L<sup>-1</sup>. This method showed good replicability and sensitivity, with limits of quantification of 3.6 ng L<sup>-1</sup> for α-HCH, 2.3 ng L<sup>-1</sup> for β-HCH, 0.9 ng L<sup>-1</sup> for γ-HCH and 5.0 ng L<sup>-1</sup> for δ-HCH. The relative standard deviation of 12 consecutive injections of a 1 mg L<sup>-1</sup> standard was 2.1 % for α-HCH, 1.3 % for β-HCH, 1.4 % for γ-HCH and 17 % for δ-HCH. Reagents are included in supplementary material (SM.1.).

## 2.4. Gas phase biosorption experiment

The gas phase biosorption of HCH was assessed by active indoor air sampling based on a solid phase extraction (SPE) system ([Barro et al., 2005](#); [Barro et al., 2006](#)). The application of this methodology to moss is novel. In this method, a known volume of air was pumped through a glass tube containing a mixture of HCH isomers and connected to two serial samplers (of ca. 30 cm<sup>3</sup> volume per sampler) with sorbent: the first with moss tissues (or Florisil® as control) and the second with Florisil®. Thus, the HCH-polluted air passed through the moss and any HCH not retained by the moss remained in the Florisil® in the second sampler. The experimental conditions were established according to previous experiments (data not published): the air was pumped at a rate of 20 L min<sup>-1</sup> for 50 min (i.e. 1 m<sup>3</sup> air), and 10 µL of a stock mixture of HCH isomers of 10 µg mL<sup>-1</sup> was added; between 0.1 and 0.2 g sorbent was used per sampler to obtain an equivalent volume of sorbent. Sampling was carried out in triplicate. The sorbents were then extracted with 2 mL of ethyl acetate in an ultrasound bath (J. P. Selecta SA) for 10 min at 25 °C and 50 Hz, and the resulting extract was filtered through hydrophobic PTFE syringe filters (0.22 µm). A surrogate was previously added to the sorbents to test the performance of extraction. The extracts obtained were then analyzed in a GC-MS-system: a Trace 1310 gas chromatograph coupled to a triple quadrupole mass spectrometer (TSQ

8000) with an IL 1310 autosampler (Thermo Scientific) (San Jose, CA, USA). Target compounds were separated on a Zebron ZB-Semivolatiles (30 m × 0.25 mm id × 0.25 μm film thickness) GC column, supplied by Phenomenex (Torrance, CA, USA). The helium carrier flow was 1.0 mL min<sup>-1</sup>. The GC oven temperature was programmed to increase from 120 °C (held 2 min) to 200 °C at 20 °C min<sup>-1</sup> and to 290 °C at 10 °C min<sup>-1</sup>. The total run time was 13 min. The injector was operated in pulsed split/splitless mode (200 kPa, held 1.2 min). The injector temperature was set at 260 °C, and the injection volume was 1 μL. The temperature of the transfer line and of the ion source were maintained at 290 and 350 °C, respectively. Selected reaction monitoring (SRM) acquisition mode was implemented, monitoring two or three transitions per isomer for an unequivocal identification and quantification of the target compounds (SM.2.). Xcalibur 2.2 and Trace Finder 3.2 software were used to operate the equipment and identify and quantify the compounds. For reagents, see supplementary material SM.1.

## 2.5. Data analysis

The amount of HCH adsorbed to the moss in the liquid phase experiment was calculated as the difference between the equilibrium concentration in the presence and absence (control) of the moss. This corrects the effect of HCH loss by volatilization or adsorption to surfaces and prevents overestimation of HCH retained by the moss. Sorption curves were constructed by plotting the cumulative adsorbed concentration of HCH in each moss versus the concentration of HCH present in the solution at equilibrium. Experimental data were fitted to the Linear (Eq. (1)) and Freundlich (Eq. (2)) models:

$$q = K_D C \quad (1)$$

$$q = K_F C^{1/n} \quad (2)$$

where  $q$  (mg g<sup>-1</sup>) is the amount of HCH adsorbed on the moss at equilibrium;  $C$  (mg L<sup>-1</sup>) is the HCH concentration in solution at the equilibrium;  $K_D$  (L g<sup>-1</sup>) is the coefficient of distribution in the Linear model;  $K_F$  (L<sup>n</sup> mg<sup>1-n</sup> g<sup>-1</sup>) and  $1/n$  (unitless) are the Freundlich coefficients.

OriginPro Software was used for fitting the experimental data to the Linear and Freundlich models, and the adjusted  $r^2$  and the  $p$ -value of the Chi-Square test for the two models were compared. In addition, Pearson regression coefficients were calculated for the affinity coefficient ( $\log K_F$  or  $\log K_D$ ) and the following: i) the  $n$ -Octanol/Water Partition Coefficient ( $\log K_{OW}$ ) of the different HCH isomers (values after Wacławek et al., 2019); and ii) isomer sizes of HCH isomers (volumes after Silvani et al., 2019).

To study the retention of the HCH isomers by mosses from the gas phase, the recovery of HCH (expressed as a percentage) from the sorbent in the first and second sampler was considered.

## 3. Results

### 3.1. Molecular characterization

The Py-GC-MS chromatograms of *S. palustre* and *F. antipyretica* are shown in Fig. 1.A, and a detailed description of the peaks detected is included in SM.3. Differences between the species were observed regarding the lipid peaks: *S. palustre* contained C<sub>16</sub> and C<sub>18</sub> saturated and unsaturated fatty acids, including a C<sub>20:4</sub> polyunsaturated fatty acid tentatively identified as arachidonic acid, while the fatty acid signal was more intense in *F. antipyretica*. In addition to C<sub>16</sub> and C<sub>18</sub> saturated and unsaturated fatty acids, large peaks were observed for acetylenic fatty acids. The THM-GC-MS chromatograms of both species are shown in Fig. 1.B. (for a detailed description of the detected peaks, see SM.3). Regarding the lipids (Fig. 1.C), *S. palustre* contained large peaks of fatty acid methyl esters (FAMES), especially in the C<sub>16</sub>-C<sub>26</sub> range. On the other hand, *F. antipyretica* contained C<sub>16</sub>-C<sub>28</sub> FAMES, including the acetylenic

FAMES. Finally, the GC-MS of the TLE of the *S. palustre* sample was composed of plant sterols (e.g. sitosterol), phytol fatty acid esters, C<sub>16</sub>-C<sub>26</sub> fatty acids and some low molecular weight carbohydrates. The TLE of *F. antipyretica* contained large amounts of C<sub>16</sub>-C<sub>20</sub> fatty acids and several acetylenic acids (C<sub>18</sub>-C<sub>20</sub>), in addition to phytol fatty acid esters and sterols.

### 3.2. Histochemical characterization

In *F. antipyretica*, the staining generally resulted in a dark blue coloration, which was particularly intense in the caulid, and fainter, but clearly observed, in most phyllids, especially in dead cells (Fig. 2A). In mature phyllids, staining was observed in the walls of both living and dead cells, with a few exceptions (Fig. 2.B(i) and 2.B(ii)). Staining of the cell cytoplasm was occasionally observed, and it was quite irregular, although intense (Fig. 2.B(i), 2.B(ii) and 2.C). By contrast, in young phyllids, in which the cuticle is still undeveloped, the cell walls were not stained, and the dye was only retained in the cytoplasm, apparently in the plastids (Fig. 2.D). Staining of *S. palustre* generally yielded fainter coloration (Fig. 2E), particularly in the caulids, which appeared transparent, almost unstained; in general, the dark appearance of some areas is due to surface curvature and not to staining, as in the case of the phyllid margins. The Sudan Black B staining was mainly restricted to the walls of cells with cytoplasm (sometimes dead), in both chlorocysts and as yet undifferentiated cells, being weaker in the latter (Fig. 2.F). Occasionally some isolated cells showed intense staining (cell indicated by an arrow in Fig. 2.F). However, in hyalocysts the walls usually remained unstained (Fig. 2.G), although a thin blackish film was occasionally observed (Fig. 2.H(i) and 2.H(ii)).

### 3.3. Liquid phase batch biosorption experiment

Adsorption isotherms were used to evaluate the biosorption of HCH by the moss tissues in water. The  $\alpha$ -,  $\beta$ -,  $\gamma$ -, and  $\delta$ -HCH curves for the two mosses species are shown, along with the experimental data and the results of fittings to Linear and Freundlich adsorption models, in Fig. 3. Overall, both the order of retention of isomers ( $\delta$ -HCH >  $\gamma$ -HCH >  $\alpha$ -HCH >  $\beta$ -HCH) and the proportion of each relative to the  $\Sigma$ HCH retained (55–61 %, 29–24 %, 16–13 % and 2 %, for  $\delta$ -,  $\gamma$ -,  $\alpha$ -, and  $\beta$ -HCH, in *F. antipyretica* and *S. palustre* respectively) were quite similar for both species. However, there were some notable differences in the retention of the different isomers and species. For *F. antipyretica*, the amount of HCH isomers adsorbed tended to increase with the increase in the concentration of HCH added, although the maximum adsorption capacity of the moss tissues was not reached under the experimental conditions (a slight decrease in the retention of  $\delta$ - and  $\gamma$ -HCH was observed in the last additions). The adsorption capacity of *S. palustre* was much lower than that of *F. antipyretica* (almost four times lower at the end of the experiment) and reached saturation with  $\delta$ -HCH on the 4th addition, with  $\gamma$ -HCH, on the 5th addition, with  $\alpha$ -HCH on the 6th addition and with  $\beta$ -HCH on the 10th addition. This explains the difference in the data for both species observed in Fig. 3.

With few exceptions, the percentage of variance in the moss HCH concentration explained by the HCH added was higher than 70 %, and in almost a third of the cases, it was higher than 90 %. For model reliability, adjusted determination coefficients and the  $p$ -value for the Chi-Square test were compared (Fig. 3). The Freundlich model provided a better fit for the sorption data, except for  $\alpha$ - and  $\beta$ -HCH in *F. antipyretica*. *F. antipyretica* showed higher affinity for HCH isomers because the  $K_D$  and  $K_F$  values were higher than for *S. palustre* (Fig. 3,  $K_D$  between 2.3 and 6 times higher and  $K_F$  between 4 and 5.5 times, except for  $\alpha$ -HCH, for which they were quite similar). The low  $K_D$  and  $K_F$  values (<1) indicated the very low affinity of this species. Ranking of affinities for each isomer differed between species:  $\delta$ -HCH >  $\beta$ -HCH >  $\alpha$ -HCH  $\approx$   $\gamma$ -HCH in *F. antipyretica*; and  $\alpha$ -HCH >  $\delta$ -HCH >  $\gamma$ -HCH >  $\beta$ -HCH in *S. palustre*. For both species, rankings of isomer affinities did not follow the same order



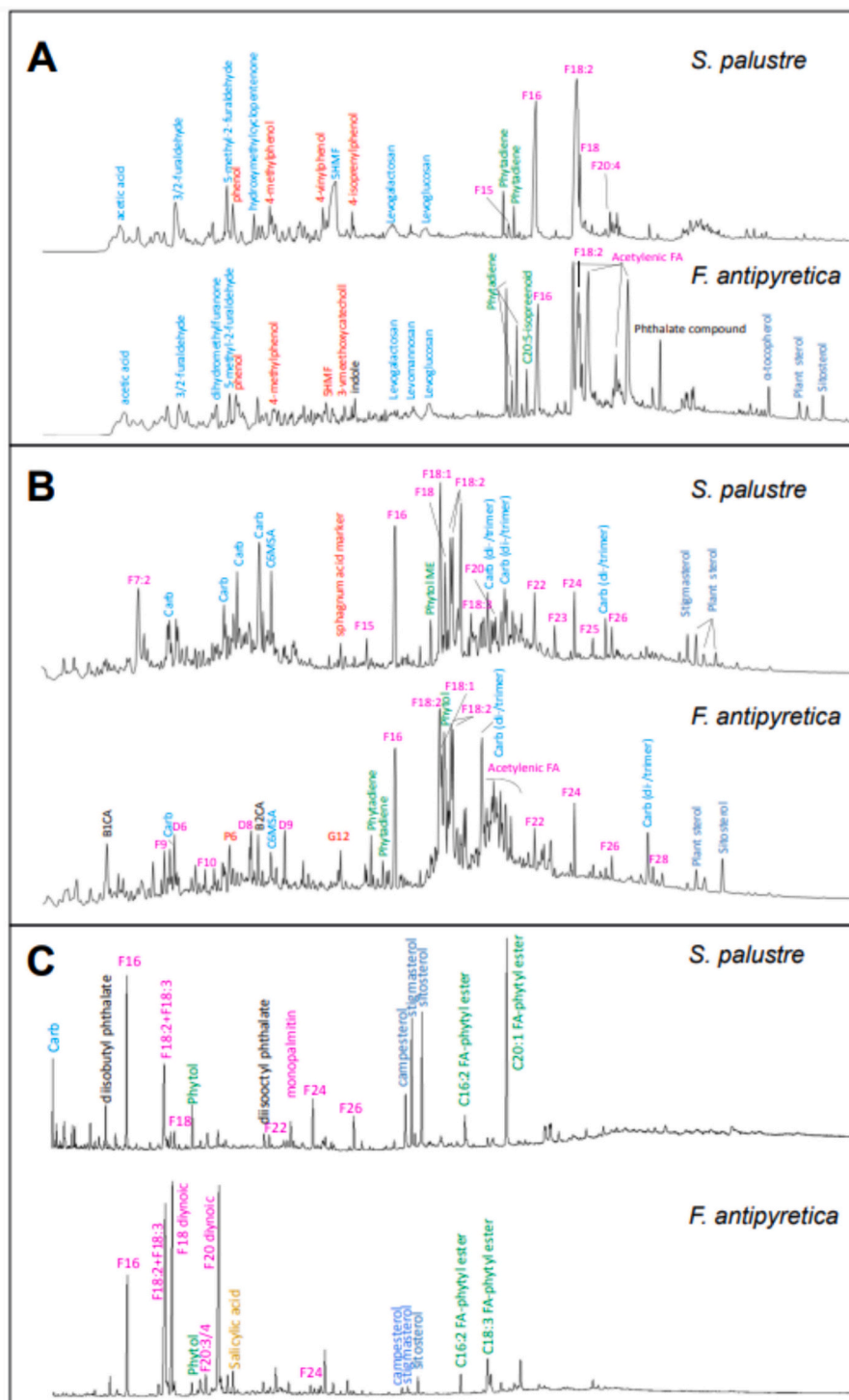


**Fig. 1.** A) Py-GC-MS total ion chromatogram traces for *Sphagnum palustre* and *Fontinalis antipyretica* bulk samples. Fatty acids, numbered according to chain length and double bonds, are shown in purple. Polyphenol products are shown in red. Carbohydrate products (5HMF = 5-hydroxymethylfuraldehyde) are shown in light blue. Plant terpenoids and sterols are shown in dark blue. Chlorophyll products are shown in green. B) THM-GC-MS total ion chromatogram traces of bulk samples. Methylated fatty acids (F) and diacids (D), numbered according to chain length and double bond, are shown in purple. Polyphenol products (P6 = 4-methoxybenzoic acid methyl ester, P12 = 3,4-dimethoxy-hydrocinnamic acid methyl ester) are shown in red. Unidentified carbohydrate products (“carb”) and a methylated C6-metasaccharinic acid (C6MSA) are shown in light blue. Plant sterols are shown in dark blue. Chlorophyll products are shown in green. B1CA-B2CA = benzene-carboxylic acids with 1–2 ester groups are shown in black. C) Total ion current chromatograms after GC-MS of total lipid extracts. Methylated fatty acids (purple), numbered according to chain length and double bonds, are shown in purple. Carbohydrates (“carb”) are shown in light blue. Chlorophyll-derived products are shown in green. Plant sterols are shown in dark blue. ME = methyl ester or ether.

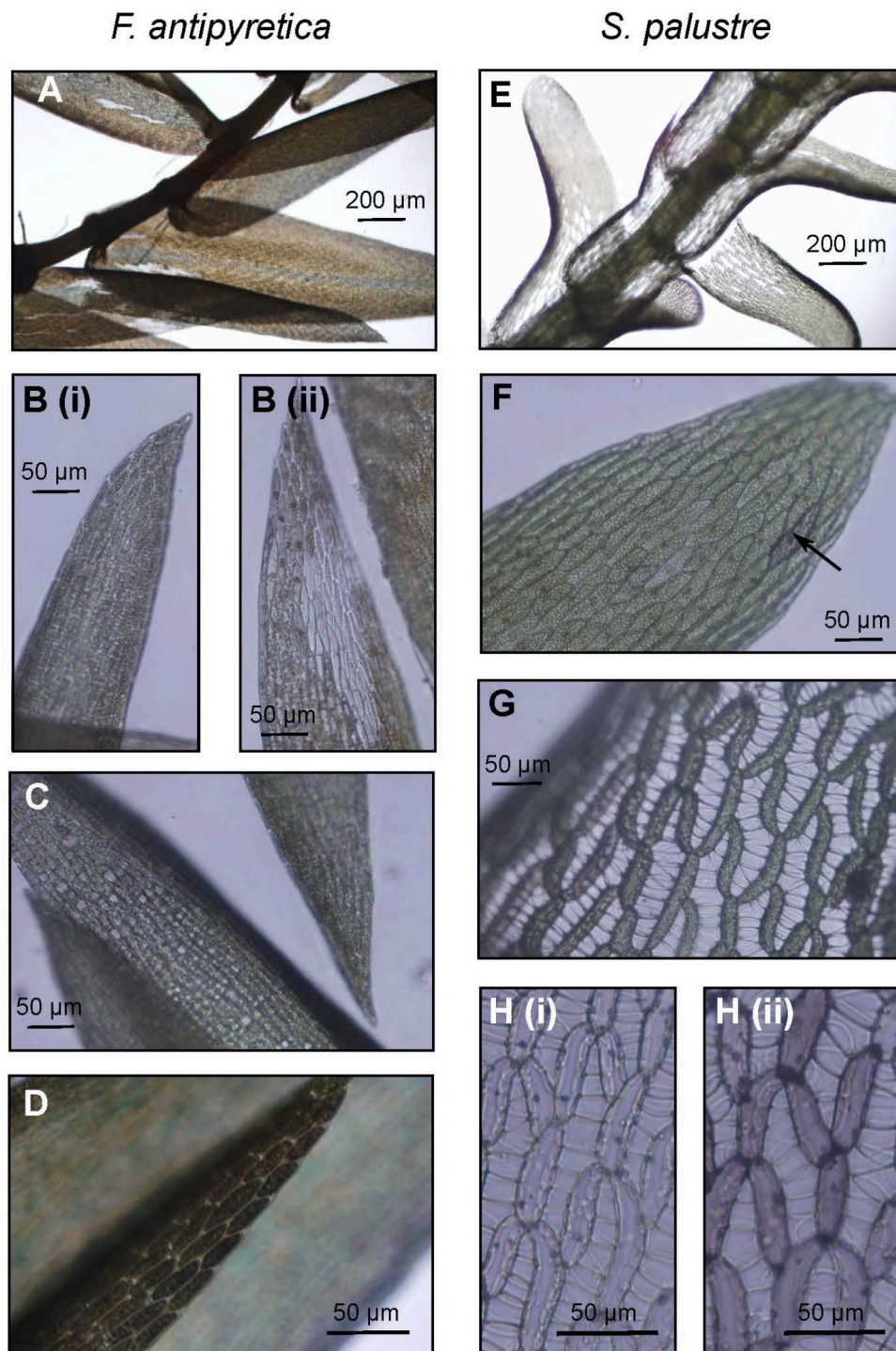


**Fig. 2.** *Fontinalis antipyretica* (A to D) and *Sphagnum palustre* (E to H) shoots after Sudan Black B staining. A) Heavily stained caulids, and less-intensely stained phyllid cells; dead cells stained more intensely. B(i), B(ii) and C) stained phyllid cells. D) Young phyllid with undeveloped cuticle showing cells with stained plastids in the cytoplasm. E) Unstained caulids and weakly stained phyllid cells. F) Undifferentiated phyllid cells showing weakly stained cell walls (the arrow indicates a single isolated cell with more intense staining). G) Phyllid with stained chlorocysts and unstained hyalocysts. H(i) Weakly stained chlorocysts and unstained hyalocysts. H (ii) occasionally the cell walls showed a thin, stained film.

as the concentrations of isomer added.

The relationship between the logarithms of the affinity coefficient ( $K_F$  or  $K_D$ ) and the n-Octanol/Water Partition Coefficient ( $K_{OW}$ ) was also studied. Relationships were only observed for *F. antipyretica* (see Fig. SM.1 in SM.4), with a significant regression ( $p < 0.05$ ) for  $\text{Log}K_F$  (with a slope value close to 1) and the same ranking of the variables compared in the case of  $\text{Log}K_D$ . Regressions between these affinity

coefficients and isomer sizes were also calculated but were not significant in any case.

### 3.4. Gas phase biosorption experiment

In the control (Florasil®), 100 %  $\Sigma\text{HCH}$  was recovered with very little loss of HCH to the second glass tube. Recoveries of HCH-isomers

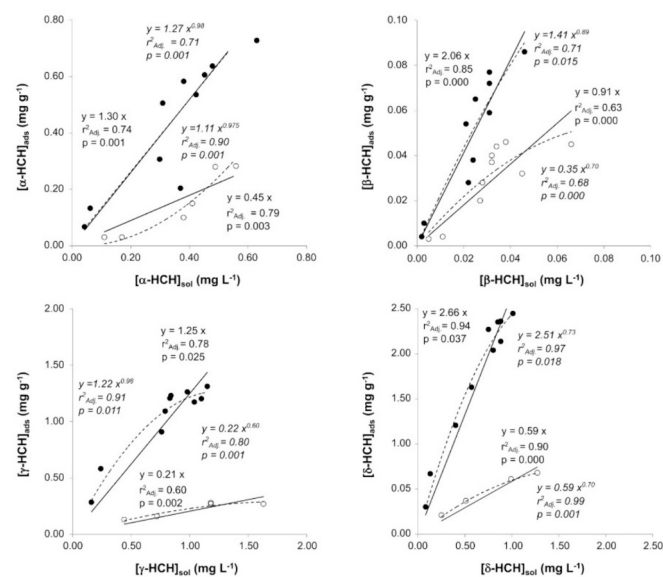


**Fig. 3.** Adsorption of individual HCH isomers on devitalized clones of the mosses *Fontinalis antipyretica* (black dots) and *Sphagnum palustre* (open dots) after 10 consecutive additions of HCH. Each dot represents the mean value of five replicates. The lines represent Freundlich (dotted lines) and Linear (solid lines) isotherms. The equations for each isotherm are also shown (Freundlich in italics, Linear in regular typeface, where  $x$  is the HCH concentration in the aqueous phase at the equilibrium ( $\text{mg L}^{-1}$ );  $y$  is the mass of solute sorbed (HCH) per unit mass of sorbent (moss) ( $\text{mg g}^{-1}$ ); constants are  $K_F$  ( $\text{mg}^{1-1/n} \text{L}^{1/n} \text{g}^{-1}$ ) in the Freundlich isotherm and  $K_D$  ( $\text{mg g}^{-1}$ ) in the linear isotherm; and the power value in the Freundlich isotherm represents  $1/n$  (intensity of the adsorption or surface heterogeneity, unitless). The adjusted determination coefficient ( $r^2_{adj}$ ) and the  $p$ -value of the Chi-Square test ( $p$ ) are also shown.

retained in Florisil® ranged between 89 and 123 %, with a low relative standard deviation (% RSD = 5–8). Notably, the isomer recoveries followed the sequence  $\delta\text{-HCH} > \alpha\text{-HCH} > \beta\text{-HCH} > \gamma\text{-HCH}$  (Table 1). The moss species exhibited different retention rates; thus, while the amount of  $\sum\text{HCH}$  retained by *F. antipyretica* was similar to the control (113 %), *S. palustre* only retained 32 % of the  $\sum\text{HCH}$  (Table 1). Different recoveries of HCH isomers were also observed. When studying *F. antipyretica*,  $\delta$ - and  $\beta$ -HCH isomers exhibited higher recoveries than  $\alpha$ - and  $\gamma$ -HCH, although all were approximately 100 %. By contrast, in *S. palustre* differences between the isomers  $\delta/\beta$  and  $\alpha/\gamma$  were more evident. Although all recoveries were <70 %,  $\alpha$ - and  $\gamma$ -HCH showed particularly low recoveries. The low recovery of  $\alpha$ -HCH (10 %) and non-existent retention of  $\gamma$ -HCH probably resulted from the transfer of these isomers into the second glass tube (97 % and 73 %, respectively) or loss within the system.

**4. Discussion**

The results of both the liquid and gas biosorption experiments indicate that *F. antipyretica* adsorbed more HCH than *S. palustre*. Based on

previous research comparing these two mosses for monitoring aquatic and atmospheric metal contamination (Debén et al., 2016; García-Seoane et al., 2023), we hypothesized that *F. antipyretica* would have a greater capacity to retain HCH in water, while *S. palustre* would be more effective at retaining HCH in the atmosphere. Nevertheless, the results of the interspecies comparison for HCH differed from those reported for metals, which apparently indicates that the loading mechanisms are completely different. Contrary to our expectations, the adsorption capacity of the aquatic moss *F. antipyretica* was higher than that of *S. palustre* in both gaseous and liquid environments and the former retained greater amounts of all HCH isomers.

The ability to adsorb lipophilic compounds such as POPs may be related to the specific surface area and the presence of lipids, mainly on the cell wall surface and the external side of the membrane. In the case of devitalised mosses, the internal surface may also be important. These different sorption capacities and the varying thresholds of HCH isomer saturation observed in the two mosses are likely to be due to species-specific factors involved in the HCH-moss interaction mechanism. Staining with Sudan Black B revealed the presence of numerous lipids (a wide variety of lipids such as protein bound lipids, phospholipids, sterols and neutral triglycerides) in the walls of most *F. antipyretica* cells (Fig. 2). By contrast, the hyalocyst of *S. palustre* did not appear to contain these compounds, and the other cells did so to a lesser extent (Fig. 2). The results of the molecular characterization of these species (Fig. 1) are consistent with the staining results, showing that the fatty acid signal is more intense in *F. antipyretica*; the higher peaks of  $\text{C}_{28}$  and acetylenic fatty acids were particularly noteworthy. Furthermore, the similarity in fatty acid patterns observed using THM-GC–MS of the bulk samples and GC–MS of the TLEs indicates that they mainly correspond to readily extractable epicuticular structures. The differences in molecular composition, which can be attributed to the epicuticular structures, can be assumed to be responsible for the differences in staining (which is consistent with the absence of staining in young *F. antipyretica* phyllids in which the cuticle is still undeveloped). These results are consistent with those of the sorption experiments: i) the liquid phase batch biosorption experiment, in which *F. antipyretica* exhibited a higher adsorption capacity and higher affinities for all the isomers (Fig. 3); and ii) the gas phase biosorption experiment, in which the result was surprising, with recoveries of approximately 100 % for all isomers in *F. antipyretica* (in all cases even higher than Florisil®) (Table 1). The latter can be attributed to the fact that this was the first time this method has been used in mosses and that these are the first data obtained for any moss species.

Regarding the adsorption processes, the best fit model in the liquid phase biosorption experiment differed between moss species and between HCH isomers (Fig. 3). For *F. antipyretica*, adsorption of  $\alpha$ - and  $\beta$ -HCH increased proportionally with the amounts of HCH added (linear isotherm), but this was not observed for  $\gamma$ - or  $\delta$ -HCH (Freundlich isotherm). This can be explained by the fact that the isotherms are usually linear at low sorbate concentrations (Delle Site, 2001), as in the case of  $\alpha$ - and  $\beta$ -HCH, with the same adsorption energy for all binding sites. Thus, the inclusion of the parameter  $1/n$  in the Freundlich equation is not necessary ( $n \approx 1$  in both cases). However, for  $\gamma$ - and  $\delta$ -HCH the value of this parameter was <1, indicating that as the solute

**Table 1**  
Efficiency of the gaseous sorption of HCH in *Fontinalis antipyretica* and *Sphagnum palustre*, expressed as percentage recovery (relative standard deviation between brackets) of the HCH added. Sampler 1 included moss tissues or Florisil® (control) and Sampler 2 only Florisil®.

Isomer	Sampler 1 (Florisil® or moss)			Sampler 2 (Florisil®)		
	Florisil®	<i>F. antipyretica</i>	<i>S. palustre</i>	Florisil®	<i>F. antipyretica</i>	<i>S. palustre</i>
$\alpha$ -HCH	96(5)	96(3)	10(4)	28(14)	19(30)	97(5)
$\beta$ -HCH	93(5)	114(8)	51(4)	6(64)	1(22)	23(42)
$\gamma$ -HCH	89(8)	111(3)	0(–)	7(51)	3(86)	73(6)
$\delta$ -HCH	123(5)	129(4)	69(7)	2(173)	0(–)	20(35)
$\sum\text{HCH}$	100(6)	113(3)	32(5)	11(34)	6(38)	53(12)



concentration increases, the adsorption energy decreases. In the case of *S. palustre*, all isomers fitted better to the Freundlich isotherm, probably due to the lower concentration at which saturation occurs relative to the other species. For  $\beta$ -,  $\gamma$ - and  $\delta$ -HCH,  $1/n < 1$ , while for  $\alpha$ -HCH, the value of this parameter was  $>1$ , indicating a different interaction between this isomer and moss. The fact that moss saturation with HCH isomers occurred at different stages suggests that there was no competition between the isomers evaluated.

Factors such as the size of the molecule and partition coefficients (Delle Site, 2001), which are related to structural differences (particularly the axial or equatorial position of the chlorine atoms; Xiao et al., 2004), can influence the interactions between the HCH isomers and the moss. Regarding the n-Octanol/Water partition coefficient, in the liquid phase batch biosorption experiment, this relationship was only fulfilled in *F. antipyrretica*, but not in *S. palustre*. By analysing the liquid phase of the same clone of *F. antipyrretica*, Carriero et al. (2021) found that PAH contents in transplants were positively correlated ( $p < 0.01$ ) with PAH solubility and negatively correlated ( $p < 0.01$ ) with  $\log K_{OW}$ . In the gaseous phase biosorption experiment, the ranking of  $\log K_{OA}$  ( $\beta$ -HCH  $\approx \delta$ -HCH  $> \gamma$ -HCH  $> \alpha$ -HCH; Wacławek et al., 2019) was consistent with the recoveries in *S. palustre*, but not in *F. antipyrretica*, in which recoveries were approximately 100 % for all isomers and ranking was therefore not possible. These results indicate that the stereochemistry of the isomer plays an important role in retention on the moss surface. Regarding the size of molecules, the lack of any significant correlations can be attributed to the similarity in size of the different isomers.

In previous passive biomonitoring studies, the concentration of HCH isomers in mosses was associated with the source of contamination and the sampling location. For instance, higher concentrations of  $\alpha$ - and  $\gamma$ -HCH (isomers with long-range transport potential) have been observed in remote areas (Borghini et al., 2005; Zhu et al., 2015). By contrast, higher concentrations of  $\beta$ -HCH were found in areas close to contamination sources (due to the high recalcitrance of this isomer in soils) (Lim et al., 2006; Tarcau et al., 2013), and in cases where HCH was still in use, higher concentrations of  $\alpha$ -HCH were detected as this the major isomer in technical HCH (Holoubek et al., 2000). The physico-chemical properties of the isomers and surface characteristics of the sorbent determine the transfer and accessibility of the pollutants. However, the original concentration determines the concentration and partitioning of isomers sorbed in mosses.

The study findings are consistent with those obtained by Keyte et al. (2009), who concluded that phenanthrene displayed a higher affinity for the cell wall components in the studied moss (*Hypnum cupressiforme*), and to a lesser extent for the membrane components. However, our findings may partly contradict those obtained by Spagnuolo et al. (2017) with the same clone of *S. palustre*, because phenanthrene adsorption mainly occurred inside the hyalocysts. By contrast, phenanthrene formed micron-sized particle aggregates, for which the hyalocysts could provide an easy route of entry, whereas the conditions of the present study refer to the liquid and gaseous phases, not to the particulate phase. These authors also observed phenanthrene on the leaf surface, which would be consistent with our results. On the other hand, live mosses were used in the previous study, unlike in the present study, and therefore some type of transport may have taken place. Thus, the importance of hyalocysts in particle loading would explain the significant relationship between the concentrations of heavier PAHs (4, 5 or 6 rings, associated with particulate matter) of the bulk deposition and the  $PM_{10}$  fraction and the moss, as reported by Aboal et al. (2020). However, this did not occur for the lighter PAHs, associated with the gaseous phase, perhaps for the same reasons as for the low affinity for gaseous phase HCHs observed in the present study (Table 1). Finally, although good uptake (proportional to the concentrations tested) was observed in the same *F. antipyrretica* clone as used for biomonitoring PAHs in inland waters under laboratory conditions, the results obtained under field conditions were not satisfactory and moss concentrations were not related to the concentrations determined in the water, although

enrichment of several PAHs was observed for several PAHs (Carriero et al., 2021). This highlights the importance of considering transport mechanisms and environmental factors in understanding differences between laboratory and field results.

## 5. Conclusions

Based on our findings, we encourage the use of *F. antipyrretica* for biomonitoring HCH in liquid and especially in gaseous phases. Cloned moss transplants of this species could be used in a simple, inexpensive and sensitive technique for quantifying, monitoring and mapping HCH in liquid and gaseous phases. Nonetheless, the performance of the moss must be tested in field studies. Confirmation of good performance would yield an inexpensive, attractive technique, which could be used simultaneously for the monitoring of other pollutants (potentially toxic elements, other POPs, etc.), including particulate matter. Thus, further information about the contributions of the different phases to the loading process in moss species must be obtained, especially under field conditions, to enable a better understanding of the variables that affect the process and improve the interpretation of the results obtained. We also consider the need for further research regarding the efficacy of other moss species, selected on the basis of high lipid contents, for adsorbing HCH. Finally, the novel methodology used in the gaseous phase biosorption experiment opens up the possibility of using other organic pollutants and different moss species.

## CRedit authorship contribution statement

**Z. Chaos:** Writing – original draft, Formal analysis, Data curation. **J. A. Fernández:** Conceptualization, Validation, Resources, Writing – review & editing, Visualization, Funding acquisition. **M. Balseiro-Romero:** Writing – review & editing, Methodology, Conceptualization. **M. Celeiro:** Writing – review & editing, Methodology. **C. García-Jares:** Writing – review & editing, Methodology, Funding acquisition. **A. Méndez:** Investigation. **P. Pérez-Alonso:** Investigation. **B. Estébanez:** Methodology, Writing – review & editing, Visualization, Funding acquisition. **J. Kaal:** Writing – review & editing, Methodology. **K.G.J. Nierop:** Writing – review & editing, Methodology. **J.R. Aboal:** Writing – review & editing, Visualization, Validation, Resources, Funding acquisition, Conceptualization. **C. Monterroso:** Writing – review & editing, Validation, Supervision, Resources, Funding acquisition, Conceptualization.

## Declaration of competing interest

The authors declare that they have no known competing financial interests or personal relationships that could have appeared to influence the work reported in this paper.

## Data availability

Data will be made available on request.

## Acknowledgements

This work was supported by the Governments of Spain (PID2019-107879RB-I00; PID2022-140985NB-C22) and Galicia (ED431C 2022/40; ED431B 2023/04, ED431C 2020/19) and was co-funded by ERDF (EU).

## Appendix A. Supplementary data

Supplementary data to this article can be found online at <https://doi.org/10.1016/j.scitotenv.2024.173021>.



## References

- Aboal, J.R., Concha-Graña, E., De Nicola, F., Muniategui-Lorenzo, S., López-Mahía, P., Giordano, S., Capozzi, F., Di Palma, A., Reski, R., Zechmeister, H., Martínez-Abaigar, J., Fernández, J.A., 2020. Testing a novel biotechnological passive sampler for monitoring atmospheric PAH pollution. *J. Hazard. Mater.* 381, 120949 <https://doi.org/10.1016/j.jhazmat.2019.120949>.
- Alharbi, O.M.L., Basheer, A.A., Khattab, R.A., Ali, I., 2018. Health and environmental effects of persistent organic pollutants. *J. Molec. Liquids* 263, 442–453. <https://doi.org/10.1016/j.molliq.2018.05.029>.
- Ares, A., Aboal, J.R., Carballeira, A., Giordano, S., Adamo, P., Fernández, J.A., 2012. Moss bag biomonitoring: a methodological review. *Sci. Total Environ.* 432, 143–158. <https://doi.org/10.1016/j.scitotenv.2012.05.087>.
- Barro, R., Ares, S., García-Jares, C., Llompard, M., Cela, R., 2005. A simple and fast micromethod for the analysis of polychlorinated biphenyls in air by sorbent enrichment and ultrasound-assisted solvent extraction. *Anal. Bioanal. Chem.* 381, 255–260. <https://doi.org/10.1007/s00216-004-2869-6>.
- Barro, R., García-Jares, C., Llompard, M., Bollain, M.H., Cela, R., 2006. Rapid and sensitive determination of pyrethroids indoors using active sampling followed by ultrasound-assisted solvent extraction and gas chromatography. *J. Chromatogr. A* 1111 (1), 1–10. <https://doi.org/10.1016/j.chroma.2006.01.093>.
- Beike, A.K., Spagnuolo, V., Lüth, V., Steinhart, F., Ramos-Gómez, J., Krebs, M., Adamo, P., Rey-Asensio, A.I., Fernández, J.A., Giordano, S., Decker, E.L., Reski, R., 2015. Clonal in vitro propagation of peat mosses (*Sphagnum* L.) as novel green resources for basic and applied research. *Plant Cell Tissue Organ Cult.* 120, 1037–1049. <https://doi.org/10.1007/s11240-014-0658-2>.
- Boquete, M.T., Aboal, J.R., Carballeira, A., Fernández, J.A., 2017. Do mosses exist outside of Europe? A biomonitoring reflection. *Sci. Total Environ.* 593–594, 567–570. <https://doi.org/10.1016/j.scitotenv.2017.03.196>.
- Borghini, F., Grimalt, J.O., Sanchez-Hernandez, J.C., Bargagli, R., 2005. Organochlorine pollutants in soils and mosses from Victoria Land (Antarctica). *Chemosphere* 58 (3), 271–278. <https://doi.org/10.1016/j.chemosphere.2004.07.025>.
- Bowman, B.T., 1979. Method of repeated additions for generating pesticide adsorption-desorption isotherm data. *Can. J. Soil Sci.* 59 (4), 435–437. <https://doi.org/10.4141/cjss79-050>.
- Capozzi, F., Adamo, P., Di Palma, A., Aboal, J.R., Bargagli, R., Fernandez, J.A., Lopez Mahia, P., Tretiaich, M., Spagnuolo, V., Giordano, S., 2017. *Sphagnum* palustre clone vs native *Pseudoscleropodium purum*: a first trial in the field to validate the future of the moss bag technique. *Environ. Pollut.* 225, 323–328. <https://doi.org/10.1016/j.envpol.2017.02.057>.
- Carrieri, V., Fernández, J.A., Aboal, J.R., Picariello, E., De Nicola, F., 2021. Accumulation of polycyclic aromatic hydrocarbons in the devitalized aquatic moss *Fontinalis antipyretica*: from laboratory to field conditions. *J. Environ. Qual.* 50 (5), 1196–1206. <https://doi.org/10.1002/jeq2.20267>.
- Concha-Graña, E., Turnes-Carou, M.I., Muniategui-Lorenzo, S., López-Mahía, P., Fernández-Fernández, E., Prada-Rodríguez, D., 2004. Development of pressurized liquid extraction and cleanup procedures for determination of organochlorine pesticides in soils. *J. Chromatogr. A* 1047 (1), 147–155. <https://doi.org/10.1016/j.chroma.2004.06.114>.
- Debén, S., Fernández, A., Carballeira, A., Aboal, J.R., 2016. Using devitalized moss for active biomonitoring of water pollution. *Environ. Pollut.* 210, 315–322. <https://doi.org/10.1016/j.envpol.2016.01.009>.
- Debén, S., Aboal, J.R., Carballeira, A., Cesa, M., Fernández, J.A., 2017. Monitoring river water quality with transplanted bryophytes: a methodological review. *Ecol. Indic.* 81, 461–470. <https://doi.org/10.1016/j.ecolind.2017.06.014>.
- Debén, S., Aboal, J.R., Giráldez, P., Varela, Z., Fernández, J.A., 2019. Developing a biotechnological tool for monitoring water quality: in vitro clone culture of the aquatic moss *Fontinalis antipyretica*. *Water* 11 (1), 145. <https://doi.org/10.3390/w11010145>.
- Delle Site, A., 2001. Factors affecting sorption of organic compounds in natural sorbent/water systems and sorption coefficients for selected pollutants. A review. *J. Phys. Chem. Ref. Data Monogr.* 30 (1), 187–439. <https://doi.org/10.1063/1.1347984>.
- Directive 2000/60/EC of the European Parliament and Council, 12 December 2000. of 23 October 2000, establishing a framework for Community action in the field of water policy. *Official Journal of the European Community L* 327, pp. 1–72.
- Fei, L., Bilal, M., Qamar, S.A., Imran, H.M., Riasat, A., Jahangeer, M., Ghafo, M., Ali, N., Iqbal, H.M.N., 2022. Nano-remediation technologies for the sustainable mitigation of persistent organic pollutants. *Environ. Res.* 211, 113060 <https://doi.org/10.1016/j.envres.2022.113060>.
- García-Seoane, R., Antelo, J., Fiol, S., Fernández, J.A., Aboal, J.R., 2023. Unravelling the metal uptake process in mosses: comparison of aquatic and terrestrial species as air pollution biomonitors. *Environ. Pollut.* 333, 122069 <https://doi.org/10.1016/j.envpol.2023.122069>.
- González, A.G., Pokrovsky, O.S., 2014. Metal adsorption on mosses: toward a universal adsorption model. *J. Colloid Interface Sci.* 415, 169–178. <https://doi.org/10.1016/j.jcis.2013.10.028>.
- González, A.G., Pokrovsky, O.S., Beike, A.K., Reski, R., Di Palma, A., Adamo, P., Giordano, S., Fernandez, J., 2016. Metal and proton adsorption capacities of natural and cloned *Sphagnum* mosses. *J. Colloid Interface Sci.* 461, 326–334. <https://doi.org/10.1016/j.jcis.2015.09.012>.
- Halvorsen, H.L., Bohlín-Nizzetto, P., Eckardt, S., Gusev, A., Moeckel, C., Shatalov, V., Pedersen Skogeng, L., Breivik, K., 2023. Spatial variability and temporal changes of POPs in European background air. *Atmos. Environ.* 299, 119658 <https://doi.org/10.1016/j.atmosenv.2023.119658>.
- Hao, Y., Li, Y., Wania, F., Yang, R., Wang, P., Zhang, Q., Jiang, G., 2021. Atmospheric concentrations and temporal trends of polychlorinated biphenyls and organochlorine pesticides in the Arctic during 2011–2018. *Chemosphere* 267, 128859. <https://doi.org/10.1016/j.chemosphere.2020.128859>.
- Harmens, H., Foan, L., Simon, V., Mills, G., 2013. Terrestrial mosses as biomonitors of atmospheric POPs pollution: a review. *Environ. Pollut.* 173, 245–254. <https://doi.org/10.1016/j.envpol.2012.10.005>.
- Holoubek, I., Korinek, P., Šeda, Z., Schneiderová, E., Holoubková, I., Pacl, A., Triska, J., Cudlin, P., Čáslavský, J., 2000. The use of mosses and pine needles to detect persistent organic pollutants at local and regional scales. *Environ. Pollut.* 109 (2), 283–292. [https://doi.org/10.1016/S0269-7491\(99\)00260-2](https://doi.org/10.1016/S0269-7491(99)00260-2).
- Jensen, W.A., 1962. *Botanical Histochemistry. Principles and Practice*. Freeman, San Francisco, USA, 408 pp.
- Keyte, I., Wild, E., Dent, J., Jones, K.C., 2009. Investigating the foliar uptake and within-leaf migration of phenanthrene by moss (*Hypnum Cupressiforme*) using two-photon excitation microscopy with autofluorescence. *Environ. Sci. Technol.* 43 (15), 5755–5761. <https://doi.org/10.1021/es900305c>.
- Kim, K.H., Kabir, E., Jahan, S.A., 2017. Exposure to pesticides and the associated human health effects. *Sci. Total Environ.* 575, 525–535. <https://doi.org/10.1016/j.scitotenv.2016.09.009>.
- Lim, T.B., Xu, R., Tan, B., Obbard, J.P., 2006. Persistent organic pollutants in moss as bioindicators of atmospheric pollution in Singapore. *Chemosphere* 64 (4), 596–602. <https://doi.org/10.1016/j.chemosphere.2005.11.007>.
- Łozowicka, B., Kaczyński, P., Wolejko, E., Piekut, J., Sagitov, A., Toleubayev, K., Isenova, G., Abzeitova, E., 2016. Evaluation of organochlorine pesticide residues in soil and plants from east Europe and central Asia. *Desalin. Water Treat.* 57 (3), 1310–1321. <https://doi.org/10.1080/19443994.2014.996008>.
- Ma, J., Hung, H., Tian, C., Kallenborn, R., 2011. Revolatilization of persistent organic pollutants in the Arctic induced by climate change. *Nat. Clim. Chang.* 1, 255–260. <https://doi.org/10.1038/nclimate1167>.
- Ma, Y., Yun, X., Ruan, Z., Lu, C., Shi, Y., Qin, Q., Men, Z., Zou, D., Du, X., Xing, B., Xie, Y., 2020. Review of hexachlorocyclohexane (HCH) and dichlorodiphenyltrichloroethane (DDT) contamination in Chinese soils. *Sci. Total Environ.* 749, 141212 <https://doi.org/10.1016/j.scitotenv.2020.141212>.
- Pacín, C., Martínez-Abaigar, J., Núñez-Oliveira, E., Aboal, J.R., De Nicola, F., Fernández, J.A., 2023. Polycyclic aromatic hydrocarbons (PAHs) levels in PM10 and bulk deposition using Mosspheres: a pilot study in an urban environment. *Environ. Res.* 223, 115406 <https://doi.org/10.1016/j.envres.2023.115406>.
- Rodríguez-Garrido, B., 2009. Movilidad, biodisponibilidad y degradación inducida de isómeros de hexaclorociclohexano (HCH) en suelos contaminados. Doctoral thesis. University of Santiago de Compostela.
- Silvani, L., Cornelissen, G., Hale, S.E., 2019. Sorption of  $\alpha$ -,  $\beta$ -,  $\gamma$ - and  $\delta$ -hexachlorocyclohexane isomers to three widely different biochars: sorption mechanisms and application. *Chemosphere* 219, 1044–1051. <https://doi.org/10.1016/j.chemosphere.2018.12.070>.
- Singh, S., Rawat, M., Malyan, S.K., Singh, R., Tyagi, V.K., Singh, K., Kashyap, S., Kumar, S., Sharma, M., Panday, B.M., Pandey, R.P., 2023. Global distribution of pesticides in freshwater resources and their remediation approaches. *Environ. Res.* 225, 115605 <https://doi.org/10.1016/j.envres.2023.115605>.
- Spagnuolo, V., Figlioli, F., De Nicola, F., Capozzi, F., Giordano, S., 2017. Tracking the route of phenanthrene uptake in mosses: an experimental trial. *Sci. Total Environ.* 575, 1066–1073. <https://doi.org/10.1016/j.scitotenv.2016.09.174>.
- Tarcau, D., Cucu-Man, S., Boruvkova, J., Klanova, J., Covaci, A., 2013. Organochlorine pesticides in soil, moss and tree-bark from North-Eastern Romania. *Sci. Total Environ.* 456–457, 317–324. <https://doi.org/10.1016/j.scitotenv.2013.03.103>.
- Tørseth, K., Aas, W., Breivik, K., Fjaeraa, A.M., Fiebig, A., Hjellbrekke, A.G., Lund Myhre, C., Solberg, S., Yttri, K.E., 2012. Introduction to the European Monitoring and Evaluation Programme (EMEP) and observed atmospheric composition change during 1972–2009. *Atmos. Chem. Phys.* 12 (12), 5447–5481. <https://doi.org/10.5194/acp-12-5447-2012>.
- UNEP, 2009. Report of the Conference of the Parties of the Stockholm Convention on Persistent Organic Pollutants on the Work of its Fourth Meeting. UNEP/POPS/COP.4/38. <http://chm.pops.int/Programmes/NewPOPs/DecisionsRecommendation/s/tabid/671/language/en-US/Default.aspx>.
- Usmani, Z., Kul, M., Lukk, T., 2021. Bioremediation of lindane contaminated soil: exploring the potential of actinobacterial strains. *Chemosphere* 278, 130468. <https://doi.org/10.1016/j.chemosphere.2021.130468>.
- Varela, Z., Boquete, M.T., Fernández, J.A., Martínez-Abaigar, J., Núñez-Oliveira, E., Aboal, J.A., 2023. Mythbusters: unravelling the pollutant uptake processes in mosses for air quality biomonitoring. *Ecol. Indic.* 148, 110095 <https://doi.org/10.1016/j.ecolind.2023.110095>.
- Vega, M., Romano, D., Uotila, E., 2016. Lindane (persistent organic pollutant) in the EU. Directorate General for Internal Policies. Policy Department C: Citizens' Rights and Constitutional Affairs. Petitions (PETI), PE, p. 571.
- Vijgen, J., Abhilash, C., Li, Y.F., Lal, R., Forter, M., Torres, J., Singh, N., Yunus, M., Tian, C., Schäffer, A., Weber, R., 2011. Hexachlorocyclohexane (HCH) as new Stockholm convention POPs—a global perspective on the management of Lindane and its waste isomers. *Environ. Sci. Pollut. Res.* 18, 152–162. <https://doi.org/10.1007/s11356-010-0417-9>.
- Vijgen, J., Weber, R., Lichtensteiger, W., Schlumpf, M., 2018. The legacy of pesticides and POPs stockpiles—a threat to health and the environment. *Environ. Sci. Pollut. Res.* 25, 31793–31798. <https://doi.org/10.1007/s11356-018-3188-3>.
- Vijgen, J., de Borst, B., Weber, R., Stobiecki, T., Forter, M., 2019. HCH and lindane contaminated sites: European and global need for a permanent solution for a long-time neglected issue. *Environ. Pollut.* 248, 696–705. <https://doi.org/10.1016/j.envpol.2019.02.029>.
- Wacławek, S., Silvestri, D., Hrabák, P., Padil, V.V.T., Torres-Mendieta, R., Wacławek, M., Černík, M., Dionysiou, D.D., 2019. Chemical oxidation and reduction of

- hexachlorocyclohexanes: a review. *Water Res.* 162, 302–319. <https://doi.org/10.1016/j.watres.2019.06.072>.
- Wöhrenschiemmel, H., Tay, P., von Waldow, H., Hung, H., Li, Y.F., MacLeod, M., Hungerbühler, K., 2012. Comparative assessment of the global fate of alpha- and beta-hexachlorocyclohexane before and after phase-out. *Environ. Sci. Technol.* 46 (4), 2047–2054. <https://doi.org/10.1021/es203109q>.
- Wong, F., Hung, H., Dryfhout-Clark, H., Aas, W., Bohlin-Nizzetto, P., Breivik, K., Mastromonaco, M.N., Brorström-Lundén, E., Ólafsdóttir, K., Sigurðsson, A., Vorkamp, K., Bossi, R., Skov, H., Hakola, H., Barresi, E., Sverko, E., Fellin, P., Li, H., Vlasenko, A., Zapevalov, H., Samsonov, D., Wilson, S., 2021. Time trends of persistent organic pollutants (POPs) and Chemicals of Emerging Arctic Concern (CEAC) in Arctic air from 25 years of monitoring. *Sci. Total Environ.* 775, 145109. <https://doi.org/10.1016/j.scitotenv.2021.145109>.
- Xiao, H., Li, N., Wania, F., 2004. Compilation, evaluation, and selection of physical-chemical property data for  $\alpha$ -,  $\beta$ -, and  $\gamma$ -hexachlorocyclohexane. *J. Chem. Eng. Data* 49 (2), 173–185. <https://doi.org/10.1021/je034214i>.
- Zhu, N., Schramm, K.W., Wang, T., Henkelmann, B., Fu, J., Gao, Y., Wang, Y., Jiang, G., 2015. Lichen, moss and soil in resolving the occurrence of semi-volatile organic compounds on the southeastern Tibetan Plateau, China. *Sci. Total Environ.* 518–519, 328–336. <https://doi.org/10.1016/j.scitotenv.2015.03.024>.